Dynamic design method of internal flow systems for rocket turbopumps

Takashi Shimura, Satoshi Kawasaki*, Masaharu Uchiumi*, Toshiya Kimura*, Mitsuaki Hayashi**, and Jun Matsui****

**Japan Aerospace Exploration Agency*

1, Koganezawa, Kimigaya, Kakuda, Miagi, 981-1525 Japan

***IHI Corporation*

1, Shin-nakahara, Isogo, Yokohama, Kanagawa, 235-8501 Japan

****Yokohama National University*

79-5, Tokiwadai, Hodogaya, Yokohama, Kanagawa, 240-8501 Japan

Abstract

A new dynamic design method of turbopumps is introduced in which their dynamic characteristics, in addition to their static characteristics, are taken into account and optimized in advance. In the present study, an interactive method to optimize the internal flow system and to verify the feasibility of the axial thrust balancing system is investigated. The model investigated is a two-stage centrifugal LH2 turbopump with an inducer driven by a two-stage impulse turbine. Firstly, axial thrust balancing range was confirmed, that is whether or not axial thrust balancing is capable with the selected configuration. Secondly, the leakage flow rate of every point in the internal flow system was evaluated. Finally, the stability of the axial thrust balancing system was evaluated.

1. Introduction

A new dynamic design method of turbopumps is under development. In this method, specifications of rotational speed, and of sizes and masses of pump impellers and turbine are determined first. Then, a combination of locations for the components such as impellers, bearings, seals, turbine, and spacers is optimized from the viewpoint of the dynamic characteristics of the rotor assembly with a focus on rotor radial vibration, and several candidates are selected. Next, for the several candidate combinations, in addition to optimization of the rotor diameter and the length of the rotor, optimization of the internal flow system is attempted. In the present study, an interactive method to optimize the internal flow system and to verify the feasibility of the axial thrust balancing system was investigated.
As for the static design of internal flow systems and axial thrust balancing systems for rocket turbopumps, many studies have been conducted [1-4]. The authors have previously reported [5] a precise method to predict the static characteristics of the axial thrust balancing system of a rocket engine turbopump. In the prediction, the effects of boundary layer conditions and angular momentum transported by internal flow were taken into account. As for the dynamic design of turbopumps, there are few examples. Recently, an analysis model of the dynamic characteristics of the internal flow system, including the axial thrust balancing system, has been reported [6]. The dynamic response of a liquid hydrogen turbopump was investigated using the frequency response method, and the important role of fluid compressibility was shown. The analysis model has been shown to be useful to investigate the problem of large amplitude axial vibration in a liquid hydrogen turbopump suspected of causing self-excited vibration [7]. In the analysis, one-dimensional, multi-domain system-analysis software AMESim® [8] was used. Expanding the analysis model, in the present study, the design feasibility of the combination selected from the viewpoint of radial vibration was evaluated from the viewpoint of the dynamic characteristics of the internal flow system and the axial thrust balancing system.
The investigated model is a two-stage centrifugal LH2 turbopump with an inducer driven by a two-stage impulse turbine. Firstly, the xial thrust balancing range was confirmed, that is whether or not axial thrust balancing is possible for the configuration selected. Secondly, the leakage flow rate of every point in the internal flow system was evaluated. Finally, the stability of the axial thrust balancing system was evaluated. In the case where it is impossible to balance the axial forces, another combination of component locations is selected. When possible, optimization among the leakage flow rate, the capable range of axial thrust balancing and the stability margin is conducted.

2. Design method

Figure 1 shows a flow chart of the dynamic design method developed [9]. In STEP 1, specifications of rotational speed, sizes and masses of the pump impellers and turbine are roughly determined to satisfy the engine requirements. Rotor dynamic fluid forces are also determined experimentally or analytically. Then, "design of form," which is a process to optimize the combination of locations for the components such as impellers, bearings, seals, turbine, and spacers, is undertaken. It is conducted from the viewpoint of the dynamic characteristics of the rotor assembly with a focus on the rotor radial vibration, and several candidates are selected. In STEP 2, for several superior combination candidates, matching among subsystems is conducted. Subsystems, including the internal flow systems, are optimized. If matching among the subsystems is impossible, for example, in the case of axial thrust balancing being out of range, STEP 1 is reconsidered so that this condition is satisfied. "Shaft geometry" optimization which optimizes the rotor diameter and the length of the rotor is also conducted in STEP 2. In the present study, an interactive method to optimize the internal flow system and to verify the feasibility of the axial thrust balancing system was focused on.

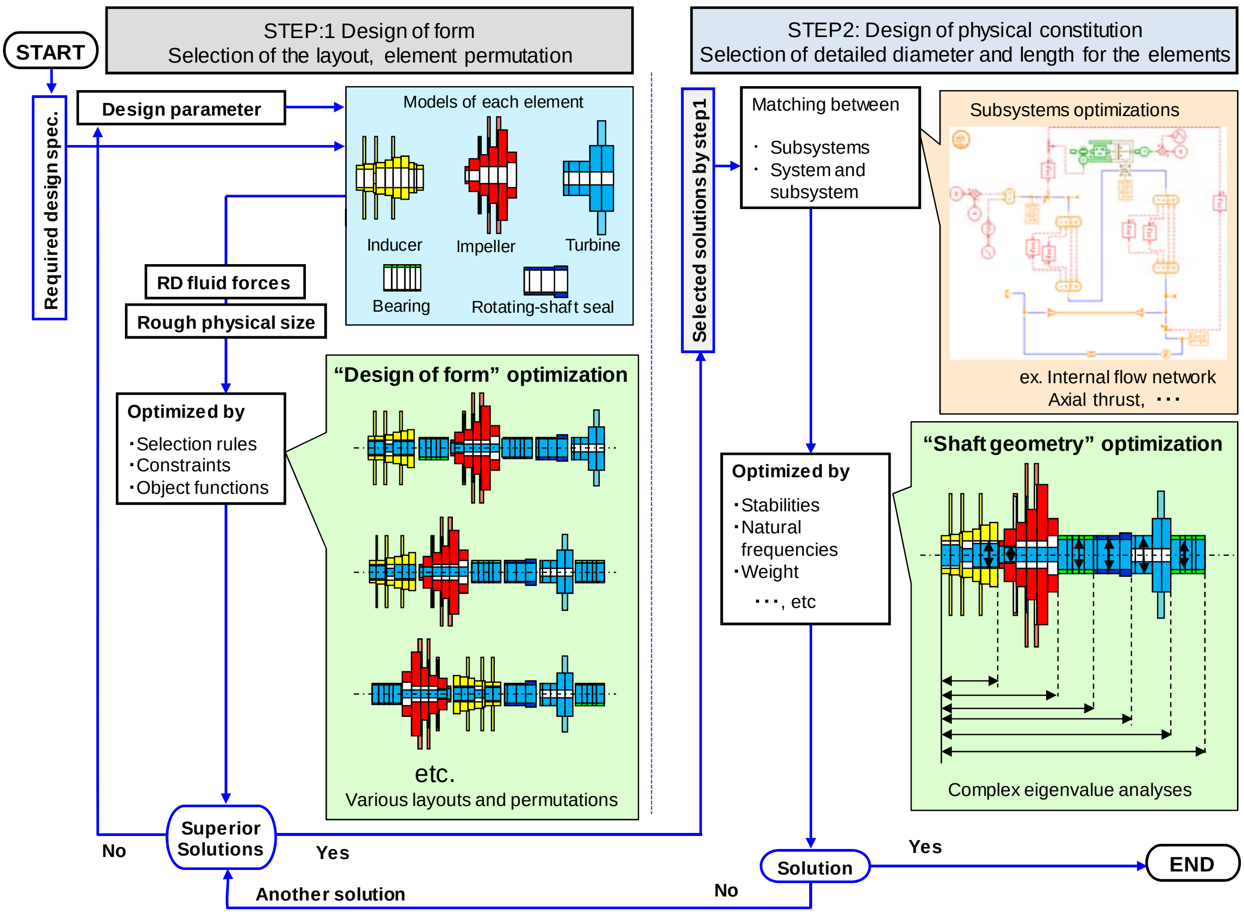

Figure 1: Flowchart of the dynamics design method

3. Analysis model

Figure 2 shows the configuration of a candidate turbopump, including the internal flow systems. The two-stage centrifugal LH2 pump with an inducer on the left is driven by the two-stage impulse turbine on the right. A balance-piston-type axial-thrust self-balancing system is installed in the turbopump using the back shroud of the 2nd impeller as the piston. Figure 3 shows the analysis model of the internal flow system and the axial thrust balancing system. The mechanical part of the balance piston and the impellers are modeled as a combination of piston sub-models corresponding to the balance piston and the side-chambers with a mass sub-model corresponding to the rotor assembly. The leakage fluid passages from the outlet of the 2nd impeller to the inlet of the 1st impeller through the balance piston were modeled with several sub-models such as variable throttling orifices, pipes, volumes, etc. The value of the piston displacement is transferred to the value of the opening areas of the #1 and #2 variable throttling orifices which correspond to the inlet and outlet orifices of the balance piston located at the back shroud of the 2nd impeller. Axial thrust generated in side chambers is modelled by pistons. Axial thrust generated in the turbine part or the inducer part is modelled by external force F. Perturbation was imposed on the outlet of the second impeller as pressure sinusoidal oscillation or pressure step. In a usual case using the model, the calculation time was less than one minute for one case.

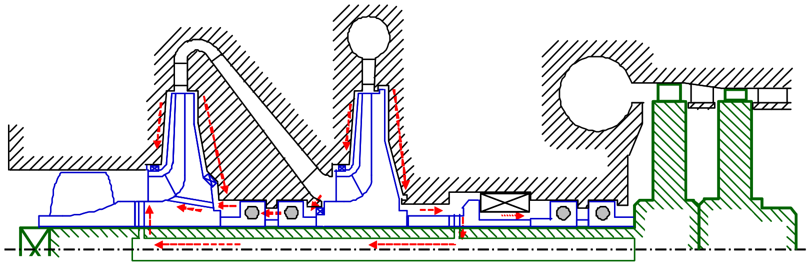

Figure 2: Configuration of the candidate turbopump (including internal flow system)

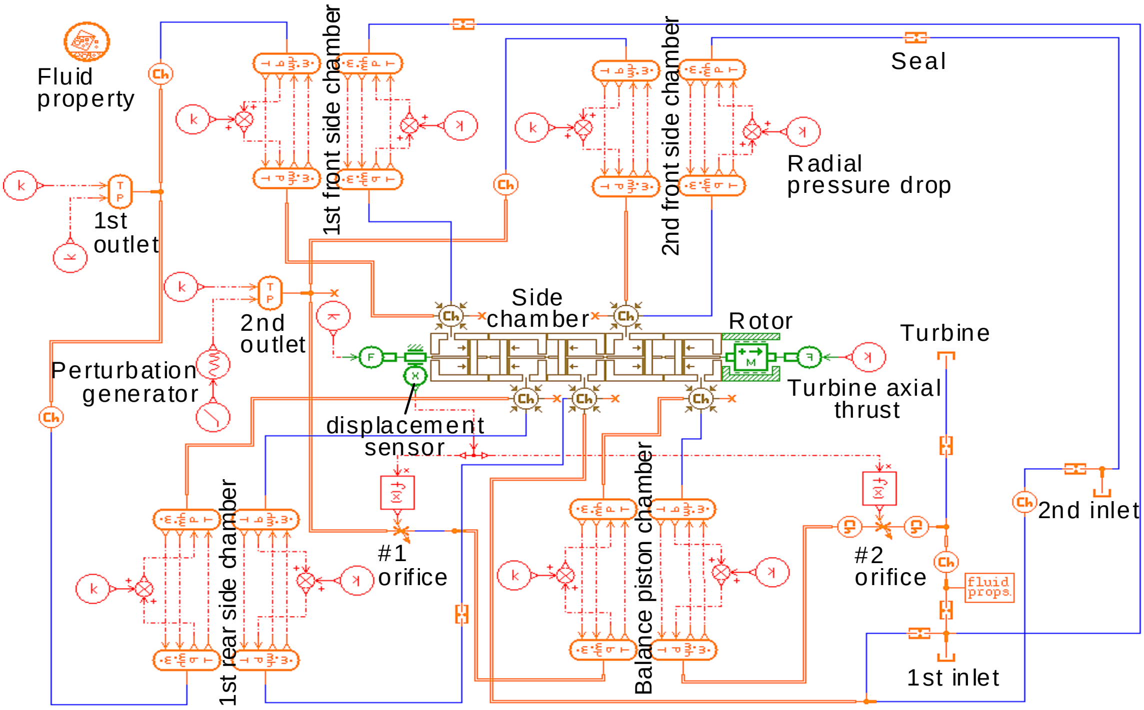

Figure 3: Analysis model of the internal flow system (AMESim chart)

4. Capable range of axial thrust balancing

Using the model shown in Fig. 3, the static characteristics of the balance piston were calculated. Figure 4 shows the calculated results. The vertical axis on the left shows axial thrust generated by the balance piston F_{bp} and that on the right shows the leakage flow rate through the balance piston Q_{bp}. In the calculation using the present code, the value of axial thrust, designated as F and "Turbine axial thrust" in Fig. 3 (the character F is reversed, simply because the sub-model F is connected reversely), generated at the turbine part was varied as a parameter. The sub-model F on the left shows the axial force generated in the inducer. For each value of F in the turbine part, the axial thrust generated by the balance piston and the balancing point of the balance piston that is the axial clearance of the #1 orifice were determined. The solid line in Fig. 4 connects the points. The rotational speed of the turbopump is 50000 rpm, the shaft diameter is 30 mm, the total axial clearance of the #1 and #2 orifices is 0.5 mm and the radial pressure drop D_{pr} in the balance piston is 2.3 MPa. The viscous damping of the piston was assumed to be 27300 N/m/s in the calculation. Parameters used in the calculations were varied for many cases. The case in Fig. 4 is determined to be the nominal case. As shown in Fig. 4, the maximum axial thrust generated by the balance piston is about 430 kN and the minimum is 80 kN within the displacement limit between 10 and 490 μ m. If the total axial thrust generated at all locations other than the balance piston is within this range, the balance piston can compensate unbalance axial thrust.

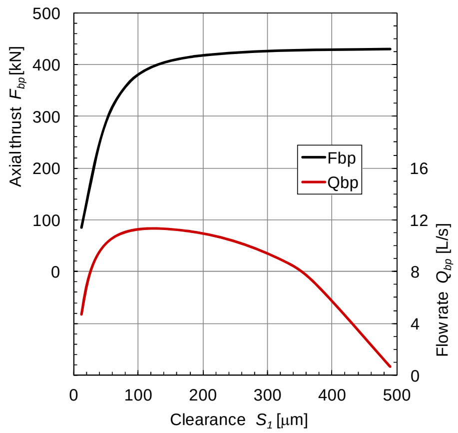

Figure 4: Static characteristics of the internal flow system (nominal case; 50,000rpm, 30mm, D_{Pr} = 2.3MPa)

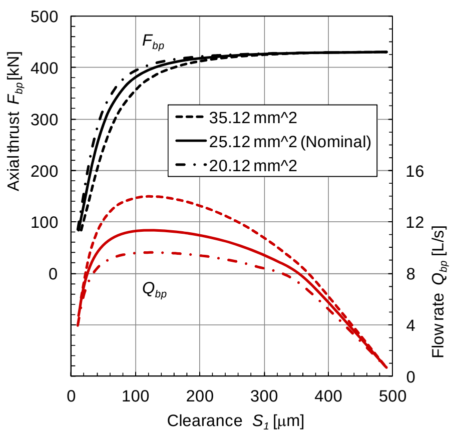

Figure 6: Effects of the downstream resistance of the balance piston

Figure 5 shows the axial thrusts generated at various locations. In this case, the turbine side axial thrust is assumed to be 120 kN and the axial thrust generated by the balance piston is calculated to be 405 kN. From the chart of Fig. 4 showing the axial clearance of #1 orifice S_1 is determined to be about 140 μ m in this case because the axial thrust of the balancing point is 405 kN. In order to maintain sufficient #1 orifice axial clearance, the axial thrust generated in the turbine part is assumed to be 120 kN in the nominal case although it is rather large for an impulse turbine.

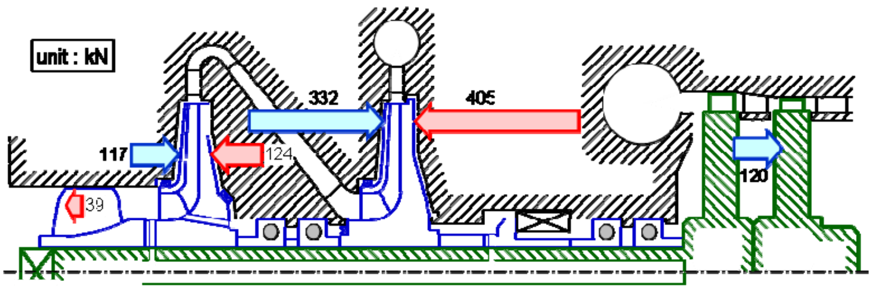

Figure 5: Axial thrust at various locations (Map of axial thrust)

5. Optimization of the internal flow system

From the view point of static performance, a wide range of axial thrust self-balancing capability and small leakage flow rate are favourable. Effects of four parameters on the static performance of the internal flow system especially for the balance piston were investigated.

5.1 Effects of downstream resistance

Figure 6 shows the effects of the downstream resistance on the static performance of the balance piston. The downstream resistance was changed parametrically by changing the area of the downstream restrictor sub-model from 20.12 mm^2 to 35.12 mm^2. With the increase of the downstream resistance due to the decrease of the area, the leakage flow rate of the balance piston decreases. This results in better volumetric efficiency. It also results in a smaller change of the #1 orifice clearance in response to the change of axial thrust other than in the balance piston because a smaller clearance change is necessary for the same amount of pressure drop at the #1 orifice in the case of a smaller leakage flow rate. In this case, the slope of Fbp curve is steeper.

5.2 Effects of total axial clearance

Figure 7 shows the effects of the total axial clearance of the #1 and #2 orifices. The total axial clearance was changed parametrically from 0.1 mm to 0.5 mm. With the increase of the total clearance, the leakage flow rate of the balance piston increases because the total resistance of the two orifices decreases. This results in worse volumetric efficiency of the pump. With the decrease of the total clearance, the slope of the F_{bp} curve becomes steeper. This affects the stability of the balance piston as mentioned later.

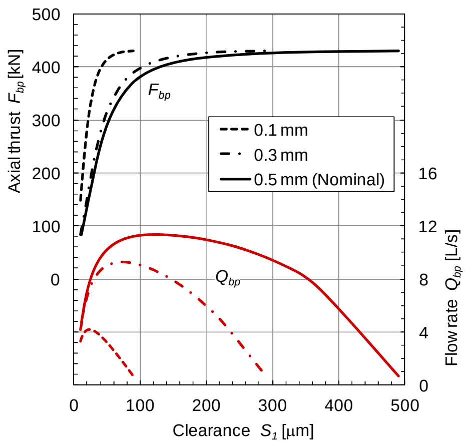

Figure 7: Effects of the total axial clearance of the balance piston

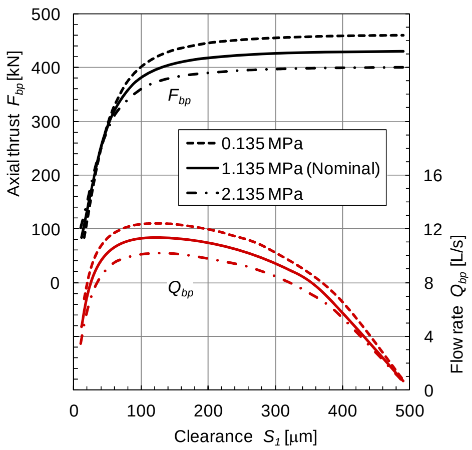

Figure 8: Effects of the radial pressure of the balance piston

5.3 Effects of radial pressure drop

Figure 8 shows the effects of the radial pressure drop in the balance piston which was varied from 0.135 MPa to 2.135 MPa. With the increase of the radial pressure drop, the leakage flow rate decreases because the drops in pressure at the #1 and #2 orifices decrease. With the increase of the radial pressure, the range of axial thrust balancing capability decreases because the minimum axial thrust generated by the balance piston increases due to the reduction of the pressure drop at the #1 orifice and that of the maximum decreases due to the reduction of pressure in the balance piston.

5.4 Effects of the 1st impeller balance holes

Without installation of the 1st impeller balance holes, the leakage flow from the inlet of the second impeller travels to the outlet of the 1st impeller because the pressure at the inlet of the 2nd impeller is higher than that at the outlet of the first impeller. This results in reverse flow in the side chamber and it is difficult to predict the radial pressure distribution there. It should also be pointed out that reverse flow in side chambers may cause instability. In order to prevent reverse flow in the side chamber, balance holes of the first impeller are effective. However, installation of the balance holes increases the leakage flow rate and results in worse volumetric efficiency. Table 1 shows the effects of the first impeller balance holes. With the increase of the balance-holes effective flow-area A, the leakage flow rate of the 1st impeller back side-chamber Q_{1r} changed from a negative value to a positive value, which means that the direction of the leakage flow was reversed. At the same time, the axial thrust generated on the back shroud of the 1st impeller F_{1r} decreased with the increase of the effective flow area of the balance holes because the pressure in the back chamber of the 1st impeller decreased. Therefore, axial thrust to pull the rotor assembly in the direction of the turbine side can be increased by installation of first impeller balance holes. This is important to control axial thrust of multi-stage turbopumps.

Table1: Effects of the 1st impeller balance hole

A [mm2]	3.91	18.91	33.91 (Nominal)	53.91
F_{1r} [kN]	134.2	129.3	124.5	121.5
Q_{1r} [L/s]	-1.78	1.75	3.07	3.63

6. Stability of axial thrust balancing system

In the previous section, static performance of the internal flow system was discussed. In this section, its dynamic performance is discussed from the viewpoint of system stability.

6.1 Effects of axial thrust other than the balance piston

To show the effects of design parameters of the internal flow system including the balance piston on the stability of the system, parametrical calculation of eigenvalues of the system operated in the vicinity of specified operating points was conducted. Figure 9 shows the effects of axial thrust other than that of the balance piston on the stability of the internal flow system by changing the axial thrust value in the turbine part. Eigenvalues are associated with a linear system of equations and are sometimes also known as characteristic roots. It is easy to conduct the eigenvalue analysis using the 1D multi-domain system simulation tool employed in the present study. The calculated results are plotted on the root locus graphs. The real part of the eigenvalues shows the damping characteristics of the roots. Their imaginary part shows the frequency characteristics of the roots. Oval shaped circles in the figure shows iso-frequency lines. Dashed lines in the figure are iso-damping-ratio lines. The first oscillating eigenvalues were located around a region a little lower than 500 Hz. The roots on the horizontal axis are not oscillating ones, namely, over damping. The roots located in the region to the right of the vertical axis are unstable because a positive value of the real part shows negative damping. As shown in the inset of Fig. 9, the turbine axial thrust was varied from -130000 N to 150000 N in the calculation. The positive value of the axial thrust shows the direction from the turbine to the pump. With the increase of the axial thrust other than the balance piston in the direction of the turbine side from the pump side, the balancing point changes and the axial clearance of the #1 orifice increases, as shown in Fig. 4. The variation rate of the axial thrust change in response to the variation of the axial displacement decreased with the increase of the axial clearance of inlet orifice #1. This variation rate is considered to be one of the feedback gains of the system and affects the stability of the balance piston system. The decrease of the variation rate tended to stabilize the system. As shown in Fig. 9, with the decrease of the axial thrust other than in the balance piston, stability of the first order oscillation increases. The first order oscillating eigenvalue moved from the region of unstable conditions to that of stable conditions.

6.2 Effects of the volume in the balance piston

Figure 10 shows the effects of the constant volume, which is attached to the balance piston and is not affected by the position of the balance piston, on the stability of the axial thrust balancing system. As shown in the box of Fig. 10, the volume was varied from 0.01 L to 0.15 L in the calculation. With the increase of this volume, the frequency of the first order vibration decreased and its eigenvalue approached the unstable region. Therefore, it is favourable to reduce the volume to increase the stability of the balance piston system.

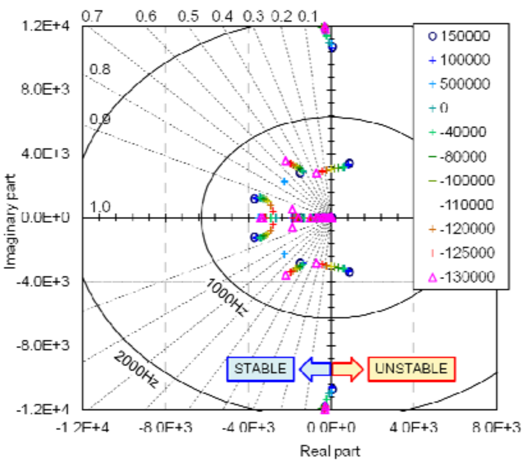

Figure 9: Effects of axial thrust other than in the balance piston

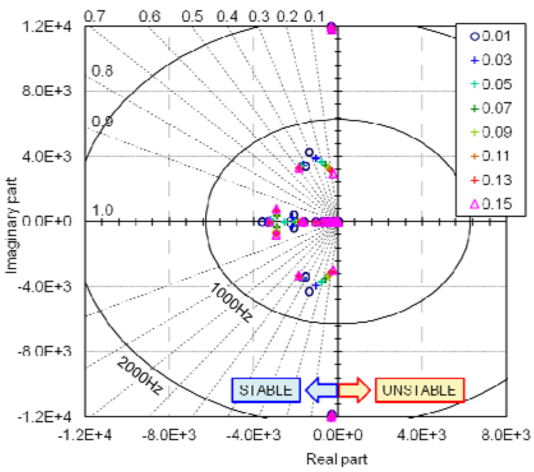

Figure 10: Effects of the volume in the balance piston

6.3 Effects of total axial clearance

Figure 11 shows the effects of total axial clearance of #1 and #2 orifices. As shown in the box of Fig. 11, the total axial clearance was varied from 0.0003 m to 0.001 m in the calculation. In the nominal case, it is 0.0005 m. With the decrease of the total axial clearance, the root approached to the unstable region. This is considered to be caused by the fact that the gain of the balance piston defined as the variation rate of the axial thrust change in response to the variation of the axial displacement increases with the decrease of the total axial clearance, as shown in Fig. 7.

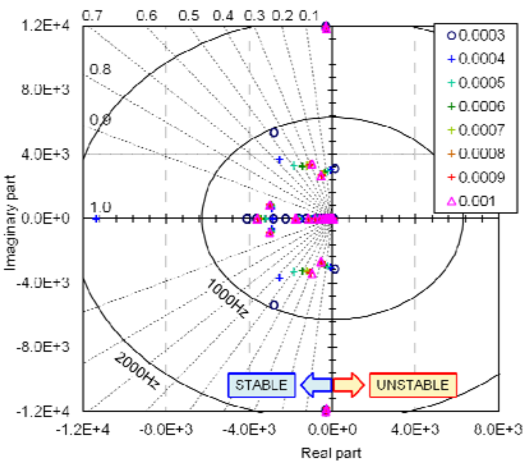

Figure 11: Effects of the total axial clearance of the balance piston orifices

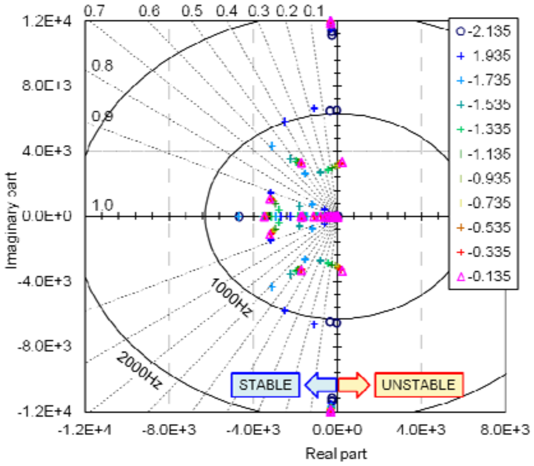

Figure 12: Effects of the radial pressure drop in the balance piston orifices

6.4 Effect of radial pressure drop

Figure 12 shows the effects of the radial pressure drop between the inlet orifice and the outlet orifice of the balance piston. As shown in the inset of Fig. 12, the radial pressure drop was varied from -2.135 MPa to -0.135 MPa in the calculation. The minus sign of the parameters shows pressure drop from the #1 orifice outlet to the #2 orifice inlet. With the decrease of the radial pressure drop, the root of the first order oscillation entered the unstable region. Installation of radial grooves on the stationary wall of the balance piston reduces the whirl of the flow in the side chamber and it results in a smaller radial pressure drop in the side chamber. As shown in Fig. 8, a smaller radial pressure drop expands the capable range of axial thrust balancing of the balance piston, but the stability of the balance piston system becomes worse at the same time.

6.5 Effects of 1st impeller balance hole

Figure 13 shows the effects of the 1st impeller balance hole. As shown in the inset of Fig. 13, the effective flow area of the 1st impeller balance hole was varied from 18.91 mm^2 to 53.91 mm^2 in the calculation. Effects are not large, but with the increase of the balance hole effective flow area, the first order root became more stable. This is thought to be caused by the fact that the gain of the balance piston defined as the axial thrust change rate to the #1 orifice clearance change decreases with the increase of that clearance. Due to the reduction of the axial thrust generated by the pressure on the back shroud of the 1st impeller, the axial clearance of the #1 orifice increases and the gain decreases.

6.6 Effects of downstream resistance

Figure 14 shows the effects of the downstream resistance of the balance piston. The downstream resistance was changed by the variation of the effective area of the restrictor. As shown in the inset of Fig. 14, the effective area of the restrictor was varied from 20.12 mm^2 to 35.12 mm^2 in the calculation. The first order root which is located at a little less than 500 Hz was scarcely affected by the resistance downstream.

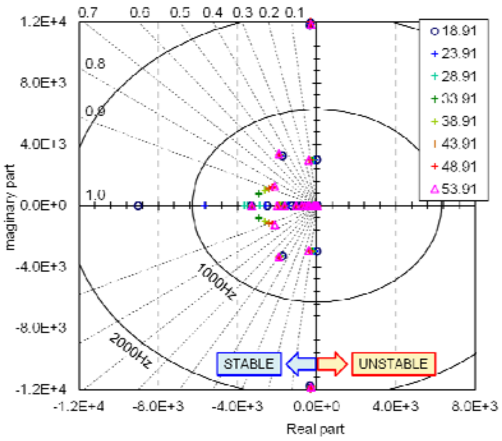

Figure 13: Effects of the 1st impeller balance hole

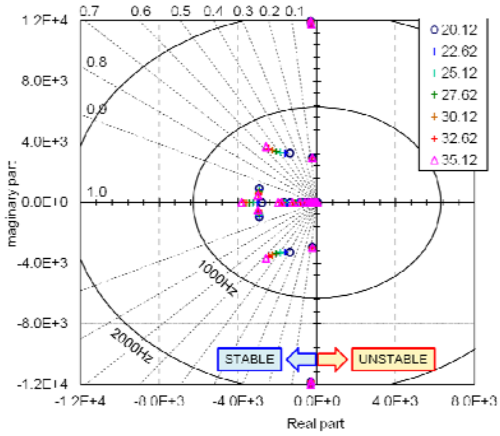

Figure 14: Effects of the downstream resistance of the balance piston

7. Conclusion

In the process of the new design method, characteristics of internal flow systems, including the axial thrust self-balancing system, were investigated both as to static aspects and dynamic aspects by the one-dimensional multi-domain system analysis software AMESim®. The conclusions are as follows:

1. By static analysis using the analysis tool, the capability of axial thrust self-balancing and the effects of various parameters on the volumetric efficiency of the model turbopump were clarified.
2. By dynamic analysis using the analysis tool, the effects of various parameters on the stability of the internal flow systems, including the balance piston, and conditions which make the system unstable were clarified.
3. The analysis model used in the present study was confirmed to be useful as part of the new dynamic design method for rocket turbopumps.

References

[1] Furst, R. B. 1973. Space Shuttle Main Engine Turbopump Design. SAE 730926.
[2] Shimura, T. and Kamijo, K. 1988. Axial Thrust t Balancing of High-Pressure Rocket Pumps. Proceedings of The Sixteenth International Symposium on Space Technology and Science. 297-302.
[3] Shimura, T., Yoshida, M., Hasegawa, S., and Watanabe, M. 1995. Axial Thrust Balancing of the LE-7 LOX Turbopump. Transactions of the Japan Society for Aeronautical and Space Sciences. Vol. 38. No. 119. 66-76.
[4] Kurokawa, J., Kamijo, K., and Shimura, T. 1994. Axial Thrust Behaviour in LOX-Pump of Rocket Engine. Journal of Propulsion and Power. Vol. 10. No. 2. 244-250.
[5] Shimura, T., Kawasaki, S., Uchiumi, M., Kimura, T., and Matsui J. April 2012. Internal Flow and Axial Thrust Balancing of a Rocket Pump. J Fluids Eng- Trans ASME. Vol. 134. 041103-1-8.
[6] Shimura, T., Kawasaki, S., Uchiumi, M., Kimura, T., Hayashi, M. and Matsui J. 2012. Dynamic Response of an Axial Thrust Balancing System for Rocket Pumps. Proceedings of ISROMAC-14. ID-1178.
[7] Shimura, T., Kawasaki, S., Uchiumi, M., Kimura, T., Hayashi, M., and Matsui J. January 2013. Stability of an Axial Thrust Self-Balancing System. J Fluids Eng- Trans ASME. Vol. 135. 01105-1-7.
[8] LMS IMAGINE S.A. 2002. How to Create Good Models without Writing a Single Line of Code. AMESim. Technical Bulletin. No. 101.
[9] Uchiumi, M., Shimagaki, M., Kawasaki, S., Yoshida, Y., and Adachi, K. 2012. Integrated Design Method of a Rocket Engine Turbopump Sub-system for Suppressing Rotor Lateral Vibration. 28th International Congress of the Aeronautical Sciences. No. 918.